NSR-05-007-060
N SG-216

American Astronautical Society: 1965 Annual Meeting

San Francisco

THE USE OF ARTIFICIAL SATELLITES FOR GEODESY[1]

William M. Kaula
Institute of Geophysics and Planetary Physics
Los Angeles, California

Artificial satellites are valuable to geodesy as elevated beacons and, through their orbit perturbations, as measures of the long wave variations of the gravitational field.

The gravitational use of satellites has now reached about the seventh degree spherical harmonics, comparable to detail of about 3,000 km in extent. The geometric use of satellites has been more limited, but now attains accuracies of about ± 0.5″ for the azimuths between tracking stations.

The current national geodetic satellite program will improve the situation somewhat by providing satellites separately optimized for geometric and gravitational purposes. With the use of further devices such as drag-free satellites, deliberately resonant orbits, and simultaneous camera directions and ranges, an eventual accuracy on the order of a couple of meters should be attainable.

INTRODUCTION

In this review we shall discuss the purposes of satellite geodesy; the principles of satellite geodesy; the results which have actually been obtained; currently planned projects; and prospects for the future.

---

[1] Publication No. 452, Institute of Geophysics and Planetary Physics, University of California, Los Angeles.

PURPOSES

The most interesting use of satellites for geodesy is scientific, because they are by far the best means of measuring long wave variations in the gravitational field which are the principal indicators of enduring departures from equilibrium in the earth. Most of the effort which has been invested in satellite geodesy has been, however, for very practical purposes. These purposes have mostly been associated with the space effort itself: the needs for accurate locations of tracking stations and accurate calculations of orbit and trajectory perturbations to calibrate tracking and guidance systems; to predict impacts and rendez-vous; to furnish accurate definitive locations for satellite-borne geophysical measurements, and photography; and to predict satellite locations for navigation. More slowly and recently satellite geodesy is being applied as a control to conventional geodesy and mapping; to locate islands and to apply a super control to the continental triangulation networks.

The greatest economic potential of satellite geodesy will be realized when it is utilized to control satellite photogrammetry. Upwards of $100 million a year is spent around the world for topographic mapping; satellite-borne photogrammetry should be capable of executing the ten percent or so of this effort which is medium scale (on the order of 1:250,000) mapping. The military applications of such systems are evident.

PRINCIPLES OF SATELLITE GEODESY

The most obvious geodetic application of a satellite is that of a very high beacon which can be seen over great distances, such as across oceans. Besides eliminating dependence on a concatenation of shorter range measurements--or attaining connections which would be impossible by the conventional techniques--satellites are attractive as a means of minimizing distortions due to atmospheric refraction, which is the principal source of systematic error in conventional geometric geodesy. This minimization is a consequence of using a target far outside most of the atmosphere: if radio signals are used, the proportionate effect of tropospheric refraction is greatly reduced; if optical signals are used, when the target is observable referred to the inertial frame constituted by the stars is also attainable. For radio tracking, there is the added complication of ionospheric refraction, which can be removed because of its frequency dependence. The radio systems used for geodetic purposes--the Navy "Transit" Doppler and the Army "Secor" CW ranging system--operate on frequencies of less than 500 Mcs, and hence transmit on multiple frequencies to enable removal of ionospheric refraction.

However, like most good things in the real world, the altitude and refraction advantages of the high satellite carry a penalty, which is that a satellite moves rather quickly: about 16,000 m.p.h., or 7 meters/millisecond. The accuracy of conventional geodesy across continents is about 1 in 300,000, so if satellites are to constitute a useful improvement we must think in terms of one-part-in-a-million accuracy. The range of a satellite at observation being around 1000 to 2000 km, this one-in-a-million thus amounts to timing accuracy of about $\pm$ .001 x 10^{-6} x 1.5 x $10^{6}/7$, or 0.2 milliseconds. Hence observations must be timed to this sort of accuracy; furthermore, we must concern ourselves either with coordinating observations thousands of miles apart to this accuracy, or with how the satellite behaves in its orbit between observations. If we choose to strive for the coordination, the obvious vehicle is the satellite itself. In the case of radio tracking requiring an accurate oscillator in the satellite--such as the "Transit" system--the satellite does prove to be an easy way to carry time accurately. In the case of radio tracking using a transponder interrogatable by several ground stations at the same time--such as the "Secor" system--it is convenient to have simultaneous observations initiated by one "master" ground station and the satellite in turn to call the other ground stations as "slaves". In the case of optical tracking, the attainment of an accurately timeable active signal visible at ranges on the order of 1500 km by cameras of reasonable mobility--say of 200 mm or less aperture--requires quite a heavy gas discharge lamp system with considerable condensers to pack enough energy into the millisecond or so flash desirable. Furthermore, the spacing of the flashes will be limited by condenser recovery capability; the number of flashes will be limited by the weight of batteries and solar cells; and the altitude of the satellite will be limited by camera sensitivity.

The short duration of flashes introduces the difficulty that the full effects of atmospheric shimmer will be felt in each satellite image, and not largely averaged out as it is in the longer exposures for stellar images. Atmospheric shimmer is something which varies considerably from place-to-place, and hence there are a variety of opinions as to its magnitude: $\pm$ 0.5″ to $\pm$ 4″, roughly. There have accordingly been developed two different schools of camera tracking. The "active" school maintains that the shimmer is small enough to make it worth the expense to instrument an active flash satellite, such as ANNA 1B or GEOS, and thus obtain the benefits of relatively cheap, mobile cameras without any timing gear. Members of the active school are the US Air Force and NASA Goddard Space Flight Center, both of whom use modifications of 1000 mm focal length f/5 aerial reconnaissance cameras. The "passive" school maintains that shimmer is large enough to make it worth the expense to instrument tracking cameras with shutters accurately timed by the VLF service, and thus obtain many images of cheap balloon-type satellites such as ECHO and PAGEOS--which are furthermore not limited in altitude to be visible. Members of the passive school are the US Coast and Geodetic Survey, which uses the 350 mm focal length f/3 ballistic cameras, and the Smithsonian Institution Astrophysical Observatory, which uses the 500 mm focal length f/1 Baker-Nunn cameras. Both these camera schools are also split another way: cameras which track to obtain more and sharper star images (NASA-GSFC and SAO); and cameras which are fixed, to avoid jitter in tracking (USAF and USC&GS). But all camera schools agree that it takes much more time and patience to obtain simultaneous observations from three or more stations than to obtain non-simultaneous observations.

The alternative to the aforedescribed difficulties is to track the geodetic satellite whenever possible, and to utilize the dynamics of the orbit to carry position from one station to another. The dynamics of the orbit must be utilized in any case to obtain information about the gravitational field from satellites.

As presumably everyone knows by now, close satellites revolve about the earth about a dozen periods per day in orbits which differ little from the Keplerian ellipse, shown in Figure 1. The principal respects in which earth satellite orbits differ from pure Keplerian are that they have nodes and perigees which revolve about one cycle in 100 days, and accelerations along the orbit which vary irregularly due to atmospheric drag and radiation pressure. The nodal and perigee precessions are due to the earth's oblateness, which is of the order 10^{-3} compared to the central term of the gravitational field. Other variations in the field are less than 10^{-5} times the

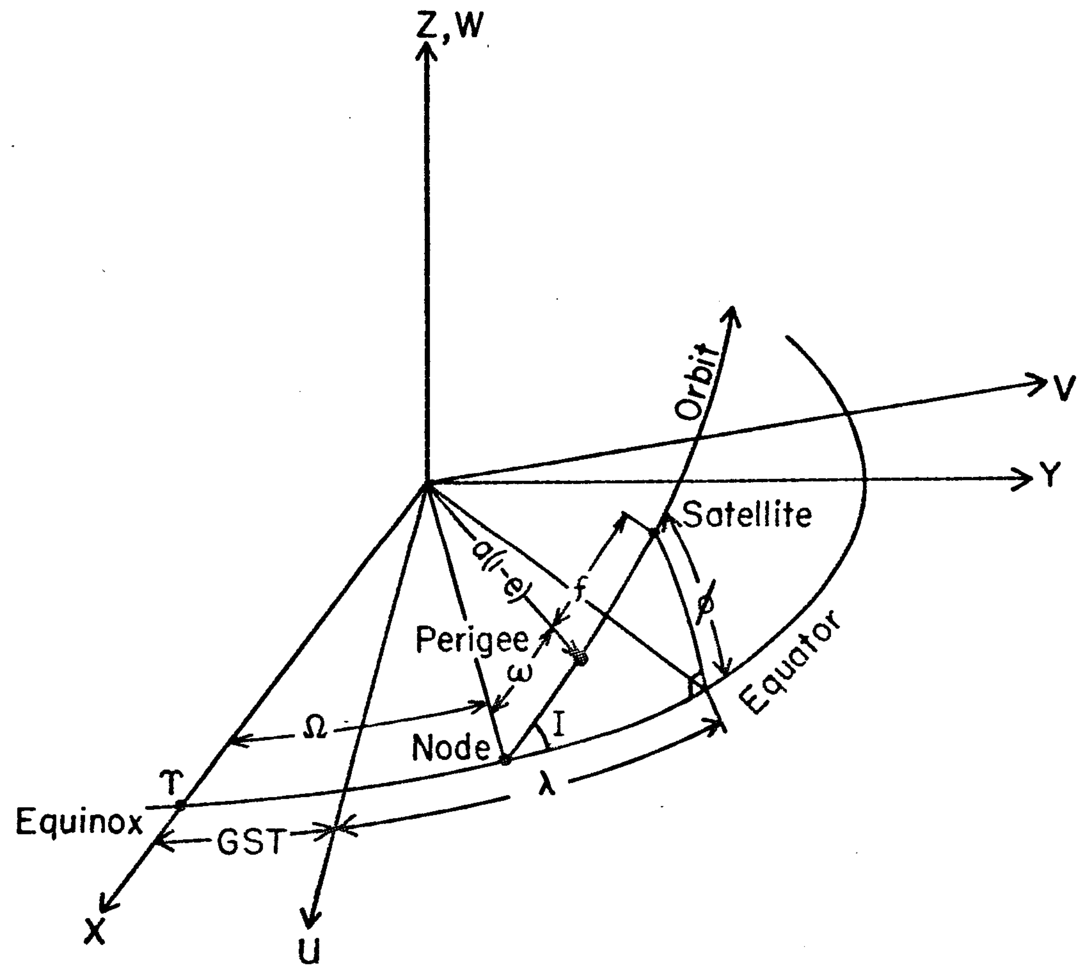

Figure 1: Coordinate systems and elements of Keplenian orbit.

central term. Hence we should expect that their effects on the orbit can be considered as forced linear oscillations about a precessing Keplerian ellipse. We should also expect that the most important effects will be those which are not excessively damped out by extrapolation to altitude, and, furthermore, are not averaged out firstly by the revolution of the satellite in its orbit and secondly by the rotation of the earth about its polar axis.

The considerations of extrapolation to altitude and the severe averaging which takes place for an object travelling as fast as a satellite in orbit suggests that a harmonic representation of the gravitational field is most convenient. Spherical harmonics--those which constitute an orthogonal set over a sphere--are expressed as

$$V_{\ell m} = GM/r \, (a_e/r)^{\ell} \, P_{\ell m} (\sin \varphi) \left[C_{\ell m} \cos m\lambda + S_{\ell m} \sin m\lambda \right], \quad (1)$$

$$0 \le m \le \ell,$$

where G is the gravitational constant; M is the earth's mass; a_e is the earth's equatorial radius; r, φ, λ are radial distance, latitude and longitude; and $C_{\ell m}, S_{\ell m}$ are the independent coefficients which we wish to determine. $P_{\ell m}(\sin \varphi)$ is the Legendre Associated Function, which is non-zero at the poles only if m is zero, and which has $(\ell - m)$ zeros along a meridian from pole to pole. Hence the higher the value of m, the more $V_{\ell m}$ represents east-west variation of the field, and the less it represents north-south. Some examples are shown in Figure 2.

The equations-of-motion of a satellite in a purely gravitational field are most compactly represented in inertially fixed rectangular position x_i and velocity $\dot{x}_i$:

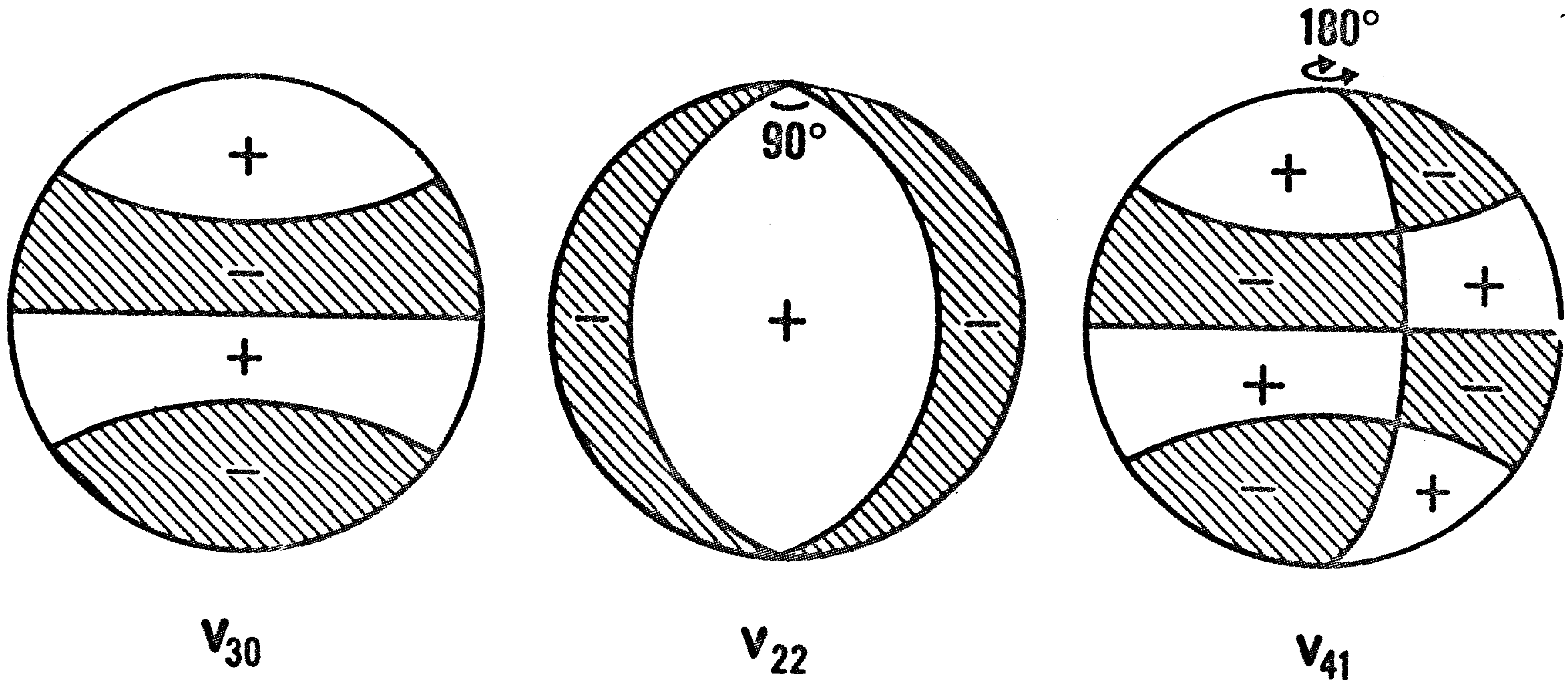

Figure 2: Examples of spherical harmonics.

$$dx_i/dt = \dot{x}_i$$
$$d\dot{x}_i/dt = -GM/r^2 + dR/dx_i, \quad i = 1, 2, 3. \qquad (2)$$

where the variations R from the central term are known as the disturbing function.

If we consider the six elements $\{a, e, I, M, \omega, \Omega\}$ (where M is now the mean anomaly, differing slightly from the true anomaly f in Figure 1) of a Keplerian ellipse which coincides in position $\underset{\sim}{x}$ and velocity $\dot{\underset{\sim}{x}}$ with a satellite as an alternative coordinate system; substitute the gravitational term $V_{\ell m}$ in (1) for the disturbing function R in (2); and convert the whole business to Keplerian elements, the equations attain the form for any one s_i of the elements

$$ds_i/dt = \sum_{p,q} f_{i\ell mpq}(a,e,I) \left[\begin{Bmatrix} C_{\ell m} \\ \text{or} \\ S_{\ell m} \end{Bmatrix} \cos A_{\ell mpq} + \begin{Bmatrix} S_{\ell m} \\ \text{or} \\ C_{\ell m} \end{Bmatrix} \sin A_{\ell mpq} \right] \qquad (3)$$

where $A_{\ell mpq} = (\ell-2p)\,\omega + (\ell-2p+q)\,M + m\,(\Omega - \theta)$, (4)

in which θ is the Greenwich Sidereal Time. If $\dot{A}_{\ell mpq}$ is non-zero, under the assumption of linearity (3) can be integrated to

$$\Delta s_{i\,\ell m} = \sum_{p,q} f_{i\ell mpq}(a,e,I) \,/\, \dot{A}_{\ell mpq} \left[\begin{Bmatrix} C_{\ell m} \\ \text{or} \\ S_{\ell m} \end{Bmatrix} \sin A_{\ell mpq} - \begin{Bmatrix} S_{\ell m} \\ \text{or} \\ C_{\ell m} \end{Bmatrix} \cos A_{\ell mpq} \right] \qquad (5)$$

The effect of the satellite motion is thus expressed mathematically by the large term $(\ell-2p+q)\,\dot{M}$ appearing in the denominator, and that of the earth's rotation by $m\,(\dot{\Omega} - \dot{\theta})$. There will always be terms of $(\ell-2p+q)$ zero which average out the satellite motion, but the effect $m\,\dot{\theta}$ is inescapable: hence tesseral harmonics (those for which the index m is non-zero) will always cause perturbations smaller in amplitude, and will be characterized by frequencies of approximately m cycles per day.

To determine the amplitude and phase angle of an oscillation such as $\Delta s_{1\ell m}$ of (5) requires observations which are well-distributed with respect to the argument $(\ell\text{-}2p)\ \omega + m\ (\Omega - \theta)$. This good distribution requires at least a distribution of tracking stations in longitude around the world; it also makes desirable a tracking system which can see the satellite through clouds and in the daylight: i.e., a radio frequency system. The two principal tracking systems which have been used for this purpose, the Smithsonian Institution Astrophysical Observatory's Baker Nunn camera system and the US Navy's Transit Doppler System (developed by the Applied Physics Laboratory of Johns Hopkins University) have, respectively, 12 and 15 stations at various locations around the world, with no gap in longitude more than about 60°, as shown in Figure 3.

As might be expected, the perturbations $\Delta s_{1\ell m}$ of the orbit by the gravitational variations are rather small, so that it is desirable not only to use as accurate tracking as possible, but also to use an orbit which maximizes the gravitational effects and minimizes the drag effects. The orbital characteristics which are most important are those Kepler elements which do not change continually: the semi-major axis, a; the eccentricity, I; and the eccentricity e. These elements appear in the transformation of the spherical harmonic $V_{\ell m}$ of (1) as coefficients of the sinusoidal variations of the form

$$GM\ a_e^{\ell} / a^{\ell+1}\ F_{\ell mp}\ (I)\ G_{\ell pq}\ (e) \qquad (6)$$

where the p and the q are the same quantities as appear in the argument $A_{\ell mpq}$ in (4). The factor (6), or its derivative, is incorporated in the factor $f_{\ell mpq}$ (a,e,I) appearing in

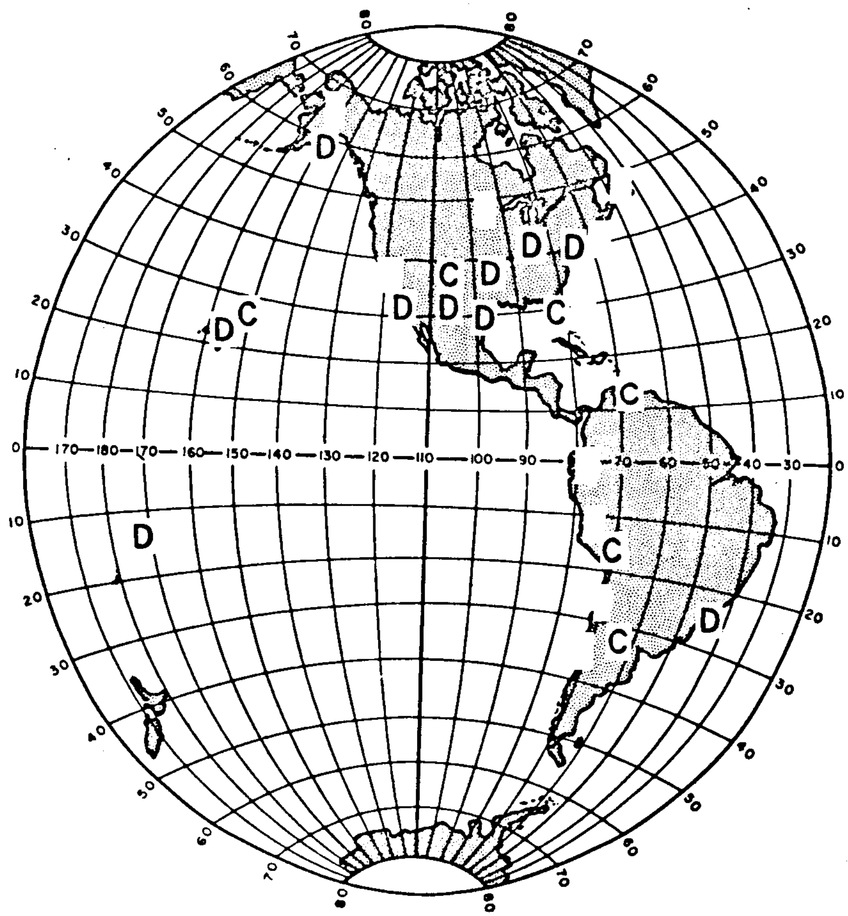

equations (3) and (5). The $1/a^{\ell+1}$ factor in (6) indicates that we want as small a semi-major axis a as possible. However, we also want a high perigee to avoid drag effects and to obtain a good distribution of observations. Since perigee radius is a(1-e), this compromise is most closely approached by having a small eccentricity e. The perigee altitude generally considered best is one at which the drag perturbations are somewhat smaller than the unavoidable radiation pressure effects--800 to 1100 km.

The order-of-magnitude of the function $G_{\ell pq}(e)$ in (6) is $e^{|q|}$. Hence if the eccentricity e is small, then the principal perturbation for which the combination $(\ell-2p+q)$ is zero is one for which p is $\ell/2$ for ℓ even and $(\ell \pm 1)/2$ for ℓ odd. Furthermore, if there are two harmonics $V_{\ell m}$ and V_{nm} of the same order m and degrees ℓ,n differing by an even number $(\ell-n)$, then the rates for their leading perturbations in a particular orbit will be the same, and they will be difficult to distinguish. The only way to resolve this ambiguity is to use a variety of orbits such that the amplitudes will vary differently; the aforestated constraints on semi-major axis a and eccentricity e require that this variety be obtained by varying the inclination I, which appears through the function $F_{\ell mp}(I)$.

It will happen that there are terms $V_{\ell m}$ for which the rate $\dot{A}_{\ell mpq}$ is very small but from which the motion in mean anomaly $\dot{M}$ is not absent--i.e.,

$$(\ell-2p)\,\dot{\omega} + (\ell-2p+q)\,\dot{M} + m\,(\dot{\Omega} - \dot{\theta}) \approx 0 \tag{7}$$

or, since $\dot{\omega}$ and $\dot{\Omega}$ are very small anyhow, we can write

$$k\,\dot{M} - m\,\dot{\theta} \approx 0 \tag{8}$$

This perturbation will have an amplified effect, because terms of the disturbing function R which contain the mean anomaly

M affect the energy of the orbit, which in Kepler elements is represented by the semi-major axis a. The semi-major axis a in turn affects the mean motion n through Kepler's law:

$$\dot{M} \approx n = \left[GM/a^3 \right]^{\frac{1}{2}} \tag{9}$$

Hence a non-zero rate $\dot{a}$ will cause an acceleration $\ddot{M}$ which if sinusoidal as in (3) will have to be integrated twice, so that the small rate $\dot{A}_{\ell mpq}$ in (7) or (8) appears squared in the denominator.

For the ideal altitudes of 800 to 1200 km and small eccentricity, $\dot{M}/\dot{\theta}$ is about 13, so if k is unity in (8) m is about 13, and the potential terms with this resonating effect are $V_{13,13}$; $V_{15,13}$; $V_{17,13}$; etc. But, in fact, these relatively high degree, short wave harmonics are the tesseral harmonics which have been most accurately determined from close satellites.

There are much more distant satellites for which the ratio $\dot{M}/\dot{\theta}$ is much smaller; however, the damping factor $1/a^{\ell+1}$ makes much smaller the zone in which the resonant amplification is perceptible. One type of such satellites are the 24-hour communications satellites SYNCOM, for which $\dot{M}/\dot{\theta}$ is close to unity.

If we are interested in station coordinates rather than variations of the gravitational field, in selecting orbital characteristics the reverse considerations of sensitivity to perturbations apply: i.e., we want the satellite to be considerably higher. Height is also desirable if we want to avoid dynamics and span oceans or continents by simultaneous techniques. The strongest geometry for networks of simultaneous observations is that which avoids small angles; hence, the optimum altitude is one which is between 0.5 and 1.0 times the gap being spanned--or 3000 to 4000 km. Satellites used in the simultaneous program of the Smithsonian's Baker-Nunn camera system have altitudes in this range, as does the balloon satellite PAGEOS which will be put up for the USC&GS's worldwide network.

RESULTS ALREADY OBTAINED IN SATELLITE GEODESY

The earliest results obtained were, of course, those dependent on the largest perturbations: the effects of zonal harmonics $V_{\ell o}$, for which the earth's rotation $\dot{\theta}$ is absent from the rate $\dot{A}_{\ell mpq}$ in (4). Several improved determinations of the oblateness term J_2 appeared in 1958, not long after satellites were first launched, closely followed by determinations of J_3, J_4, etc.. Since 1958, there has been a gradual improvement in determination of zonal harmonics from satellites, up to about the 14th degree. This improvement has been a consequence of the availability of a greater variety of orbital inclinations and of the decrease in drag effects on satellites, the latter in turn due both to the decrease in upper atmospheric density with solar activity and to the availability of higher perigee satellites. The principal recent solutions are given in Table 1.

The determination of tesseral harmonics of the gravitational field is generally quite a separate analysis from the zonals because the periodicities of the perturbations used differ by a factor of more than fifty. In the analysis for zonal harmonics, Keplerian elements averaged over a duration on the order of a week can be determined from the observations, and then the week-to-week variations of these elements can be examined to determine the zonal harmonics. In the analysis for tesseral harmonics, the periods of the perturbations used are often not much longer than the intervals between the observations. Hence osculating elements cannot be determined for short enough intervals; partial derivatives of the observations themselves with respect to the tesseral harmonic coefficients must be formed. Furthermore, the smaller amplitudes of the perturbations, the greater number of terms of perceptible effect, and the existence of station position errors of comparable magnitude to the tesseral harmonic perturbations all make the solution much more dependent on the statistical techniques, implicit as well as explicit, applied in the analysis. Consequently satellite orbit analysis to determine tesseral harmonics and station coordinates requires elaborate programs on a large scale computer, and thus has been done only at a relatively few centers. The results set forth in Table 2 were all obtained since mid-1964 and are all a great improvement over earlier results. This improvement is partly because of better tracking but more because the best satellite orbits were not attained until relatively recently: for example, as indicated by Table 3, no satellite in the 800-1200 km perigee zone near the most sensitive inclination, 90°, was launched until mid-1963. The improvement is probably due just as much to development of better techniques of analysis. The remaining discrepancies are probably due as much to differences in methods of analysis as to differences in data. For example, the coefficients of Izsak should be expected to be too small in absolute magnitude in the average, because he used an iterative technique in which he determined corrections to orbital elements of several arcs in stages alternate to determining corrections to the station positions and tesseral harmonics. Hence at any given stage non-uniform distribution of observations can cause the corrections to the orbital constants of integration to absorb some of the correction to the tesseral harmonics. Guier and Anderle both utilize a partitioning of the normal equations which enables simultaneous least squares solution incorporating any number of orbits for orbital elements and the geophysical parameters.

Also launched in 1963 was the first transmitting 24-hour satellite, SYNCOM II, which constitutes the best independent test of the results obtained from much closer satellites. The results of this test are shown in Table 4. The gravitational terms to which the 24-hour satellites are most sensitive are V_{22} and V_{33}. What makes SYNCOM a good test is that V_{33} is relatively difficult to determine from close satellites of small eccentricity. Hence the good agreement with Anderle's solution shown in Table 4 breeds confidence therein up through at least the 4th degree. The spatial representation of the gravitational field customarily employed is the geoid height: the location of the equipotential surface most nearly coinciding with mean sea level with respect to an ellipsoidal reference figure. It is calculated from a set of potential terms $V_{\ell m}$ as shown in equation (1) merely by

$$N = R \sum_{\ell,m} V_{\ell m}, \qquad (10)$$

where R is the mean radius of the earth. The geoid is thus a summation of the simple geometric forms shown in Figure 2.

Figure 4 shows the geoid corresponding to the solution of Anderle in Table 2. This representation is the one which is most suggestive geophysically; it corroborates the old observation of Jeffreys that the correlation of the long wave variations of the gravitational field with the topography is very low. The geoid height representation also enables another good independent test: the ups-and-downs over the continents should agree with those calculated by astro-geodesy: i.e., the integration over the surface of slopes of the equipotential with respect to the ellipsoid measured by the "deflections of the vertical": the discrepancies between astronomic and geodetic positions. The near satellite determinations satisfy this test considerably better than any

Figure 4: Geoid Heights in meters with respect to an ellipsoid of flattening 1/298.30. By Anderle [1965].

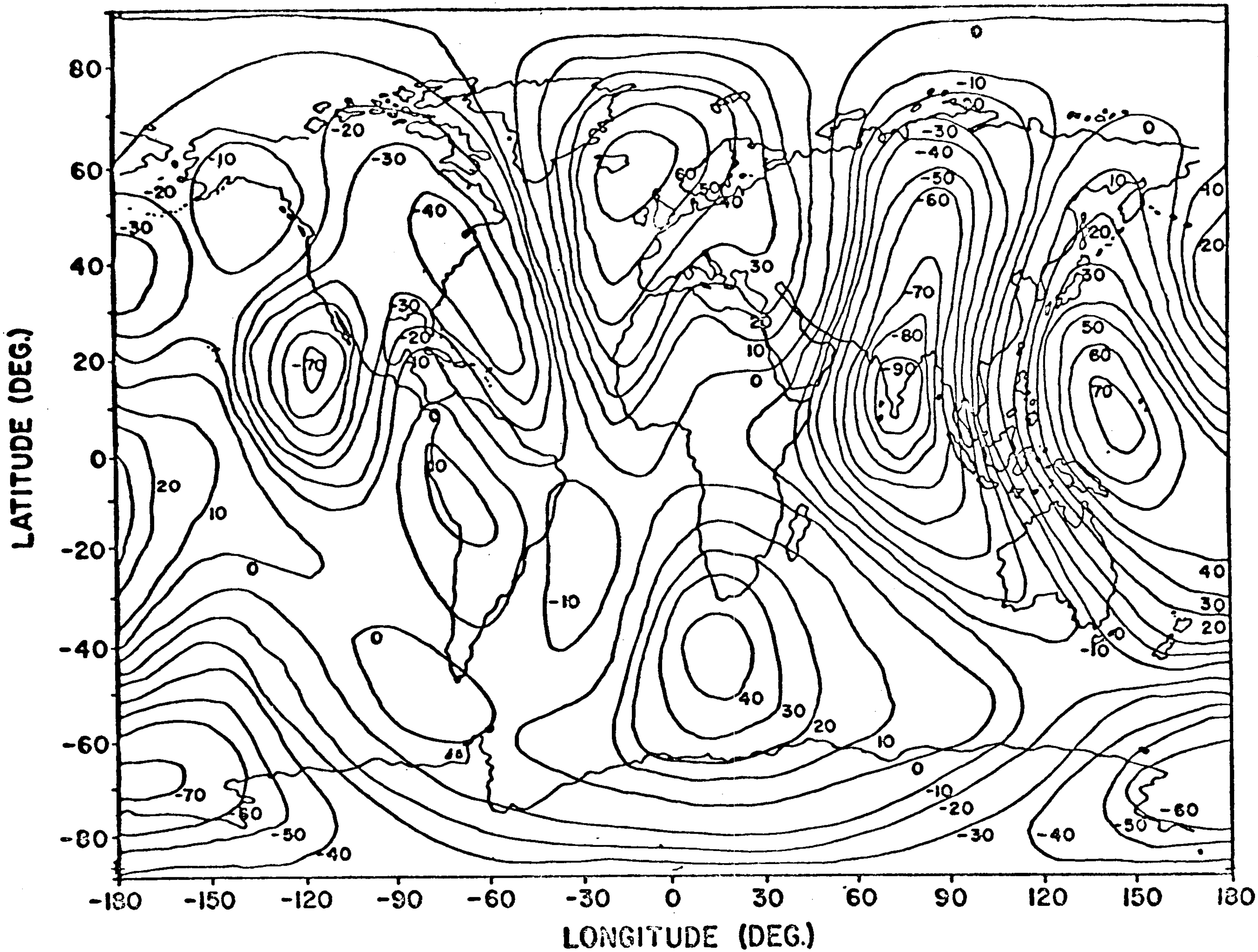

of the older gravimetric geoids.

In obtaining the by-product to analysis for tesseral harmonics of tracking station coordinate shifts, most investigators have allowed all stations to shift separately. This independent shifting of stations which may be connected to the same geodetic triangulation system is unfortunately necessitated by uncertainty as to the validity of the connection in some cases. The geodetic triangulation thus provides an independent check on relative positions of tracking stations. Such a check with Transit Doppler stations in North America yields agreement within about $\pm$ 20 meters. Of more interest is a comparison of absolute positions--i.e., coordinates with respect to the earth's center of mass. Table 5 shows such a comparison; it is expressed in terms of radial, longitudinal, and latitudinal shifts because the first two coordinates are involved in questions of systematic error. The radial coordinate of position is dependent on the definition of scale as appearing through Kepler's law, equation (9). The longitudinal coordinate of position is dependent on the definition of orientation and time. The latitudinal coordinate, however, should be free of systematic effects, and the $\pm$ 10 meters discrepancies in Table 4 should be indicator of the accuracies of the different systems.

Also amongst the dynamical contributions of space vehicles to geodesy should be mentioned the determination of GM from the lunar probes Ranger VI, VII, and VIII. A distant object is best for such determinations mainly because of the relatively great length which is actually measured; the accuracy should be essentially that of the velocity of light. The Ranger determinations yield a GM of 3.98601×10^{14} m^3/sec, about 1 in 400,000 lower than the best results by other means.

Actual results already obtained for the purely geometrical use of satellites for geodesy are more limited, since they are more dependent on satellites designed specifically for geodesy, of which only one has been launched: ANNA1B ($1962\beta\mu$), which never attained its full potentiality due to instrumental malfunction and the effect on its solar cells of artificial energetic particles from the July 9, 1962 blast. The smaller cameras--the active technique of the USAF using ANNA1B, the passive techniques of the USC&GS using ECHO I--have attained $\pm 0.5''$ to $1.0''$ agreement with geodetic triangulation for the azimuth between two tracking stations up to about 1600 km apart, which is as good as the triangulation is believed to be. The internal accuracy of the USC&GS observations indicated by the adjustment of the Mississippi--Minnesota--Maryland triangle shown in Figure 5 is about 1 in 750,000, not far short of the 1 in a million minimum accuracy desired. The large Baker Nunn Cameras of the SAO using satellites above 3000 km, such as MIDAS 4, have made more than 600 simultaneous observations for 14 pairs of stations up to 6500 km apart, as shown in Figure 6. The accuracy of the mutual azimuths indicated by internal consistency is about $\pm 0.2''$ to $\pm 0.7''$.

CURRENTLY PLANNED PROJECTS

Since the launching of ANNA 1B, responsibility for geodetic satellites has been transferred back to NASA. A national geodetic satellite program has been formulated, intended to meet the needs of all interested agencies. This intent has resulted in essentially two series of satellites: the active Beacon Explorer and GEOS satellites with altitudes around 1000 km, and the passive PAGEOS satellites with altitudes around 4000 km. Orbital characteristics and schedules of these satellites are summarized in Table 6.

The Beacon Explorer satellites are dual purpose; they carry ionospheric top-side sounding antennas, for which the 1000 km altitude is also desirable. The instrumentation of geodetic

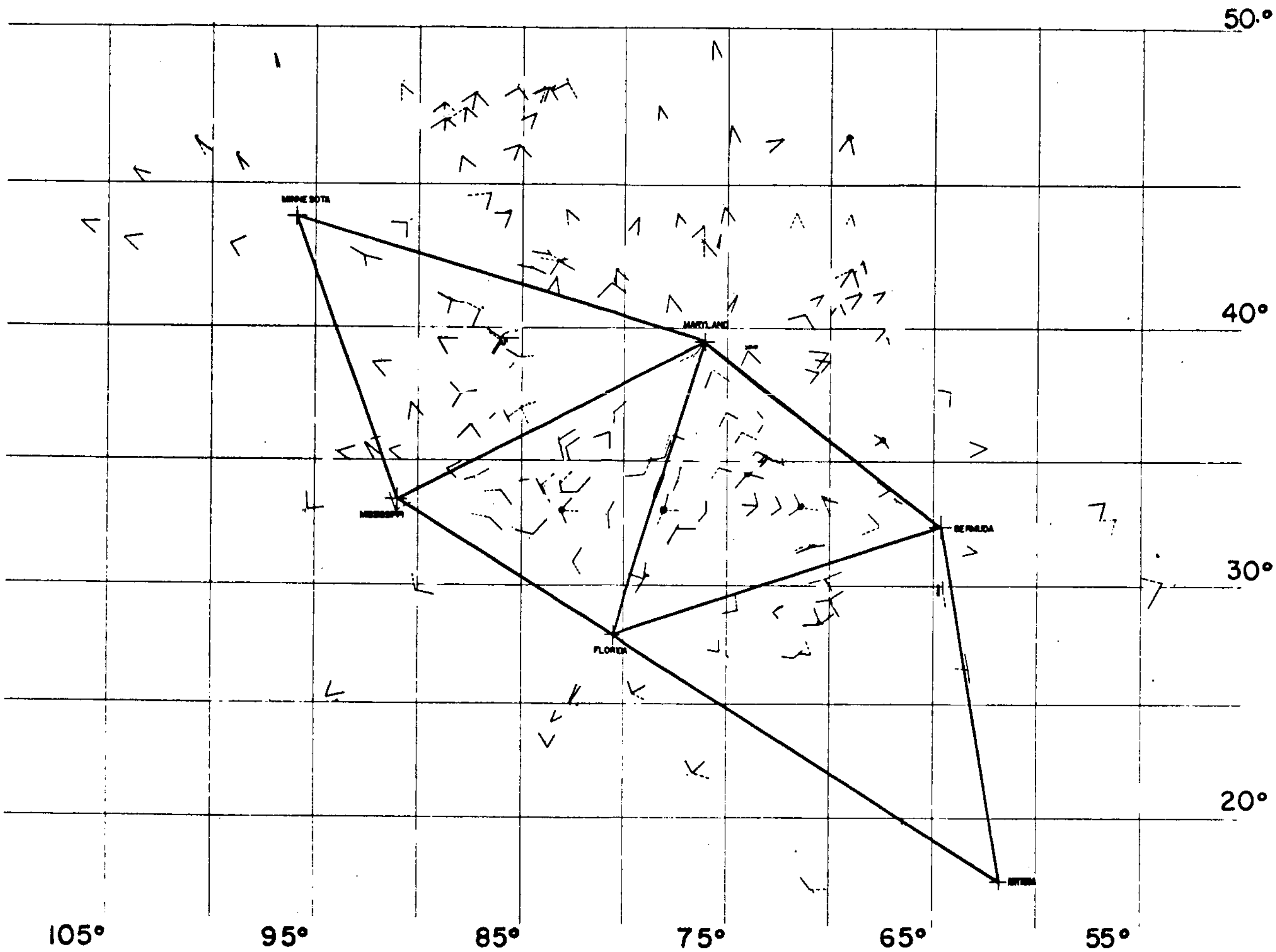

Figure 5: Simultaneous observations by the USC&GS Ballistic Cameras.

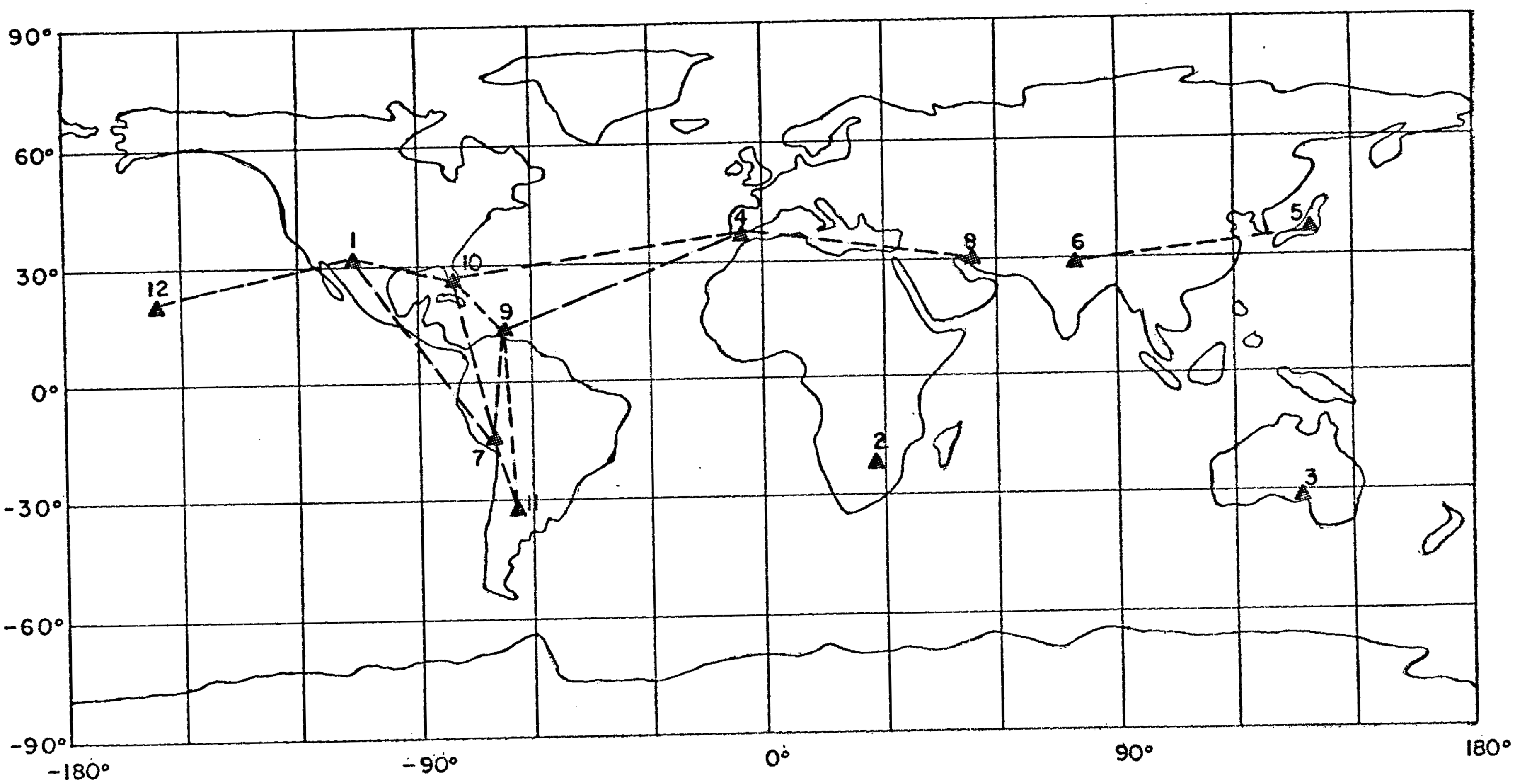

Figure 6: Simultaneous observations by the SAO Baker-Nunn Cameras.

interest comprises a Transit Doppler beacon and corner reflectors designed for use with laser searchlights.

The GEOS satellites, constructed by Applied Physics Laboratory of Johns Hopkins University, are distinguished by carrying a xenon flash lamp system, similar to ANNA 1B. The principal improvement over ANNA is the use of gravity gradient stabilization, which maintains the lamp always in a downward pointing orientation. The lamps and reflectors are also improved to yield 11,000 to 48,000 candle seconds, dependent on the angle from the central axis. The power capacity allows about 650 flashes per day. The GEOS also carries a corner reflector for laser tracking and a variety of radio tracking: the Transit Doppler beacon (transmitting at 162,324 and 648 Mcs); the Secor ranging transponder (421 Mcs up; 224 & 448 Mcs down) and the NASA--GSFC range- and range-rate transponder (2270 Mcs up, 1705 Mcs down).

A considerable complex of tracking systems will be observing GEOS. The primary users of the flashing light will be the modified 1000 mm f/5 aerial cameras: the PC-1000's of the USAF, and the MOTS' cameras of NASA. In addition, it will be observed by 300mm f/2.5 ballistic cameras of the USC&GS and DOD; the Baker Nunn cameras of SAO (for which it is too bright); plus a number of foreign stations. The laser systems tracking GEOS will be at least two, one developed by NASA--Goddard Space Flight Center and the other by USAF--Cambridge Research Laboratories. The US Army Secor stations will number about ten, most of them to be operated closely enough together to enable frequent simultaneous or near-simultaneous observations to locate islands. The NASA--GSFC range- and range-rate system comprises two fixed stations; its primary purpose is to track more distant satellites, and its tracking of GEOS will be primarily for calibration purposes.

The PAGEOS satellite will be considerably simpler than GEOS; in addition to the balloon itself, the only signal will be that from a Minitrack beacon, operating at 136 Mcs. The PAGEOS is primarily designed for the purpose of obtaining a world wide network of 36 stations with the USC&GS ballistic cameras, as shown in Figure 7. It is also too bright for the SAO Baker-Nunn cameras.

PROSPECTS FOR THE FUTURE

The improvement of determination of the gravitational field depends much more on a good variety of orbital inclinations to resolve ambiguities than on more accurate tracking. The National Geodetic Satellite program will help improve this variety, but it will still lack the inclinations which would do the most good, 10° to 20°. This lack is apparently because of their low utility to geometrical geodesy outside the tropics. It therefore seems most appropriate to launch a relatively inexpensive Doppler-only satellite in a near equatorial orbit.

An important instrumental improvement currently under development is the drag-free satellite, which comprises a proof mass, an external shield, a sensor to determine when the proof mass and the shield approach each other, and jets to re-center the shield on the proof mass. Such a satellite will follow a purely gravitational orbit, undisturbed by surface force effects. It is difficult to see how further improvement in determination of the gravitational field can be otherwise obtained after the solar activity increases again.

Another device which should be considered is a family of resonant satellites satisfying the condition expressed by equation (8). The present mode of geodetic use of satellites is rather obtuse, depending on forced oscillations; normally, an instrument is made much more sensitive to what is to be measured.

The world network in Figure 7 will be limited in accuracy to that of the star catalogues on which the camera observations depend: from $\pm$ 0.2″ in the northern hemisphere to $\pm$ 0.5″ in the most southernly latitudes is anticipated for the AGK3 system and its southern hemisphere supplement. Hence it is desirable to improve the accuracy of the PAGEOS system by measuring ranges to the satellite along with the directions obtained by camera.

The current program plus some of the afore-stated improvements should result in a measurement of most of the gravitational field through the 12th degree spherical harmonics, and of absolute positions of tracking stations to better than $\pm$ 5 meters.

REFERENCES

1. Anderle, R., "Geodetic Parameters set NWL-5E-6 based on Doppler satellite observations", Proc. 2d Int. Symp. Geod. Use of Satellites, Athens, in press, 1965.

2. Guier, W.H. and R. R. Newton, "The earth's gravity field deduced from the Doppler tracking of five satellites", J. Geophys. Res. 70, in press, 1965.

3. Hadgigeorge, G., "Numerical results from geodetic satellite ANNA optical data", Proc. 2d Int. Symp. Geod. Use of Satellites, Athens, in press, 1965.

4. Izsak, I.G., "A new determination of tesseral harmonics by satellites" in Kovalevsky, J. ed., Trajectories of Artificial Celestial Bodies as Determined from Observations, Springer Verlag, Berlin, in press, 1965.

5. Kaula, W.M., "A geoid and world geodetic system based on a combination of gravimetric, astrogeodetic, and satellite data", J. Geophys. Res., 66, 1799-1811, 1961.

6. Kaula, W.M., Theory of Satellite Geodesy, Blaisdell Publ. Co., New York, in press, 1965.

7. King-Hele, D.G. and G. E. Cook, "A new determination of the even zonal harmonics of the earth's gravitational potential" in Kovalevsky, J., ed. Trajectories of Artificial Celestial Bodies as determined from Observations, Springer Verlag, Berlin, in press, 1965.

8. King-Hele, D.G., G.E. Cook and D. W. Scott, "The odd zonal harmonics in the earth's geopotential", Proc. 2d Int. Symp. Geod. Use of Satellites, Athens, in press, 1965.

9. Kozai, Y., "Long-Range analysis of satellite observations" in Kovalevsky, J., ed. Trajectories of Artificial Celestial Bodies as determined from Observations, Springer Verlag, Berlin, in press, 1965.

10. Large, B.O., "The drag-free satellite", AIAA Journal, 3, in press, 1965.

11. Mueller, I.I., Introduction to satellite geodesy, Frederick Ungar Publ. Co., New York, 415 pp., 1964.

12. Schmid, H., "Precision and accuracy consideration for the execution of geometric satellite triangulation", Proc. 2d. Symp. Geod. Use of Satellites, Athens, in press, 1965.

13. Smith, D.E., Plan. & Space Sci., 13, in press, 1965.

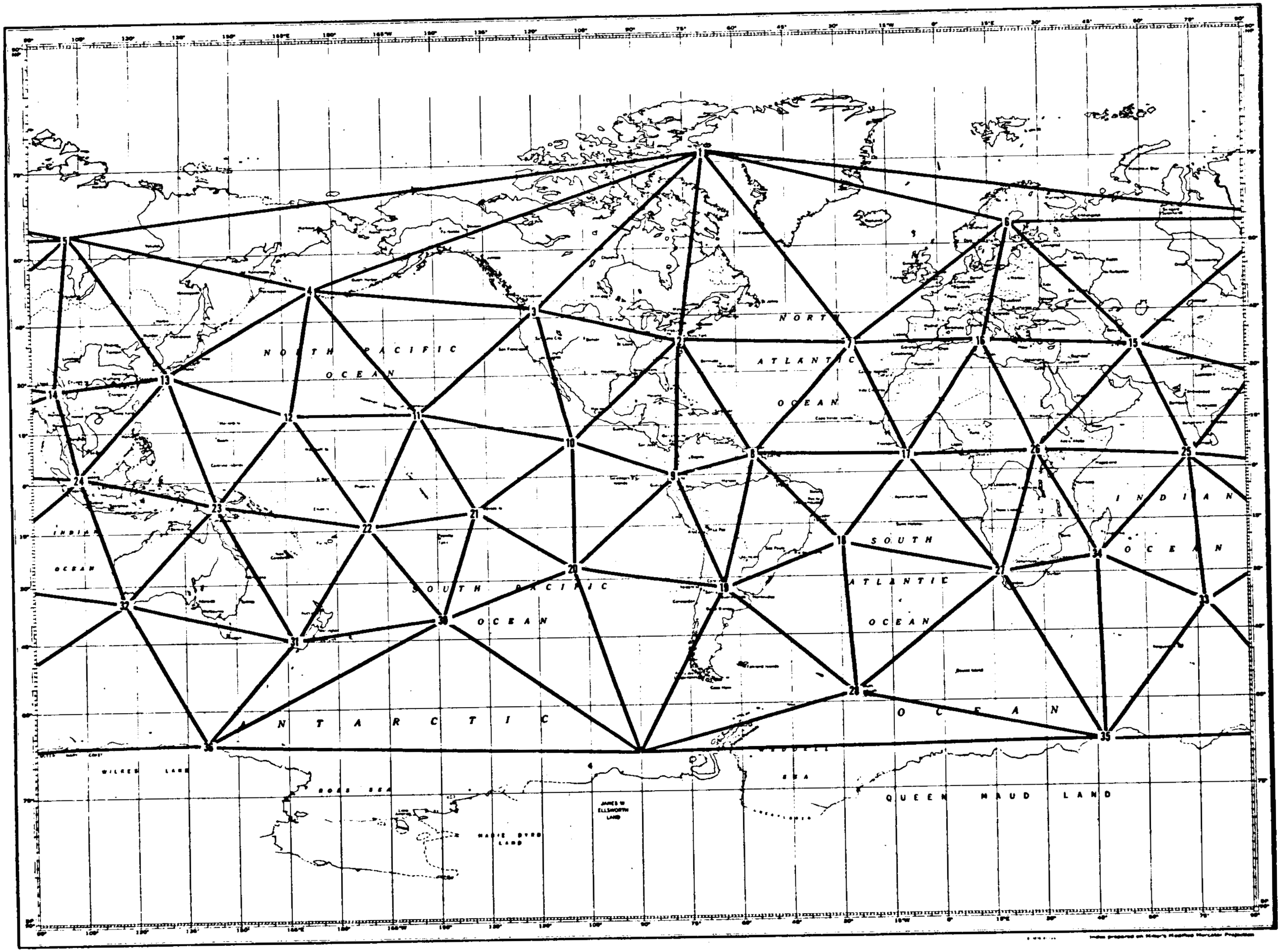

Figure 7: Planned world-wide geometric satellite network.

Table 1

GRAVITATIONAL ZONAL HARMONICS DETERMINED FROM SATELLITES

Multiply all values by a scaling factor of 10^{-6}

	Kozai [1965]	King-Hele et al [1965]	Guier & Newton [1965]	Anderle [1965]	Smith [1965]
$\bar{C}_{2,0}$	-484.174	-484.172		-484.194	-484.172
$\bar{C}_{3,0}$	0.963	0.967	1.019	0.984	0.923
$\bar{C}_{4,0}$	0.550	0.507		0.507	0.567
$\bar{C}_{5,0}$	0.063	0.045	0.002	0.045	0.054
$\bar{C}_{6,0}$	-0.179	-0.158		-0.219	-0.202
$\bar{C}_{7,0}$	0.086	0.114	0.163	0.105	0.077
$\bar{C}_{8,0}$	0.065	-0.107			0.112
$\bar{C}_{9,0}$	0.012	-0.028	-0.048		
$\bar{C}_{10,0}$	0.012				0.037
$\bar{C}_{11,0}$	-0.063				
$\bar{C}_{12,0}$	0.071				0.044
$\bar{C}_{13,0}$	0.022				
$\bar{C}_{14,0}$	-0.033				-0.035

$\bar{C}_{n,0}$ is the coefficient of the normalized zonal harmonic

$$\bar{P}_{n0}: \int_{-1}^{1} \left[\bar{P}_{n0}(x)\right]^2 dx = 2$$

$$\bar{C}_{n0} = -J_n / \sqrt{2n+1}$$

Table 2

GRAVITATIONAL TESSERAL HARMONICS
DETERMINED FROM SATELLITES

Multiply all values by a scaling factor of 10^{-6}

ℓ	m	Anderle [1965] $\bar{C}_{\ell m}$	Anderle [1965] $\bar{S}_{\ell m}$	Guier & Newton [1965] $\bar{C}_{\ell m}$	Guier & Newton [1965] $\bar{S}_{\ell m}$	Izsak [1965] $\bar{C}_{\ell m}$	Izsak [1965] $\bar{S}_{\ell m}$
2	2	2.45	-1.52	2.38	-1.20	2.08	-1.25
3	1	2.15	0.27	1.84	0.21	1.60	-0.04
3	2	0.98	-0.91	1.22	-0.68	0.38	-0.80
3	3	0.58	1.62	0.66	0.98	-0.17	1.40
4	1	-0.49	-0.57	-0.56	-0.44	-0.38	-0.40
4	2	0.27	0.67	0.42	0.44	0.20	0.58
4	3	1.03	-0.25	0.84	0.00	0.69	-0.10
4	4	-0.41	0.34	-0.21	0.19	-0.11	0.43
5	1	0.03	-0.12	0.14	-0.17	-0.14	-0.04
5	2	0.64	-0.33	0.27	-0.34	0.24	-0.27
5	3	-0.39	-0.12	0.09	0.10	-0.67	0.05
5	4	-0.55	0.15	-0.49	-0.26	-0.13	0.16
5	5	0.21	-0.59	-0.03	-0.67	0.08	-0.41
6	1	-0.08	0.19	0.00	0.10	-0.02	0.12
6	2	0.13	-0.46	-0.16	-0.16	0.05	-0.23
6	3	-0.02	-0.13	0.53	0.05	0.05	0.00
6	4	-0.19	-0.32	-0.31	-0.51	0.07	-0.39
6	5	-0.09	-0.79	-0.18	-0.50	-0.28	-0.38
6	6	-0.32	-0.36	0.01	-0.23	-0.12	-0.59
7	1	0.33	0.08	0.13	0.09		
7	2	0.35	-0.19	0.46	0.06		
7	3	0.32	0.04	0.39	-0.21		
7	4	-0.47	-0.24	-0.14	0.00		
7	5	0.05	0.02	-0.06	-0.19		
7	6	-0.48	-0.24	-0.45	-0.75		
7	7			0.09	-0.14		
8	1			-0.15	-0.05		
8	2			0.09	-0.04		
8	3			-0.05	0.22		
8	4			-0.07	-0.04		
8	5			0.08	-0.00		
8	6			-0.02	0.67		
8	7			0.17	-0.07		
8	8			-0.15	0.09		
13	13	-0.028	0.106	-0.046	0.048		
15	13	-0.054	-0.051				
15	14	0.009	-0.025				

$\bar{C}_{\ell m}, \bar{S}_{\ell m}$ are coefficients of the normalized harmonic

$$\bar{Y}_{\ell m} = \bar{P}_{\ell m} \begin{Bmatrix} \sin \\ \cos \end{Bmatrix} m\lambda$$

$$\int_{\text{sphere}} \bar{Y}^2_{\ell m}\, d\sigma = 4\pi \left\{\bar{C}_{\ell m}, \bar{S}_{\ell m}\right\} = 4\pi \left[(\ell+m)!\ /\ (\ell-m)!\ (2\ell+1)\right] \left\{C_{\ell m}, S_{\ell m}\right\}$$

Table 3

SATELLITES USED TO DETERMINE TESSERAL HARMONICS

Satellite	Tracking O:Optical D:Doppler	Launch Date	Incli- nation	Perigee-Height-Apogee km	
VANGUARD 2	O	1959 Feb 17	32.9°	559	3320
VANGUARD 3	O	1959 Sep 18	33.3°	512	3744
ECHO I ROCKET	O	1960 Aug 12	47.2°	1502	1685
EXPLORER 9	O	1961 Feb 16	38.9°	634	2583
TRANSIT 4A	O,D	1961 Jun 29	66.8°	881	998
MIDAS 4	O	1961 Oct 22	95.9°	3496	3756
TRANSIT 4B	D	1961 Nov 16	32.4°	956	1104
ANNA 1B	O,D	1962 Oct 31	50.1°	1077	1182
*1963-38C	D	1963 Sep 28	89.9°	1075	1126
*1963-49B	D	1963 Dec 5	90.0°	1057	1109

*(TRANSIT series satellites)

Table 4

ACCELERATIONS IN LONGITUDE OF 24-HOUR SATELLITES

Degrees/Day^2 x 10^{-3}

	SYNCOM II: 33° Incl.			SYNCOM III:: 0° Incl.	
	First Period	Second Period	Third Period	First Period	Second Period
Longitude	55° - 58° W	59° - 63.5° W	245° - 197.5° E	180° - 178° E	179° - 174° E
Observed	-1.27	-1.32	+1.13	+1.20	+1.07
	± .02	± .02	± .05	± .05	± .11
Calculated from coeff. of:					
Anderle (1965)	-1.26	-1.26	+1.09	+1.11	+1.03
Guier & Newton (1965)	-1.25	-1.22	+1.03	+0.82	+0.74
Izsak (1965)	-1.05	-1.06	+0.98	+0.92	+0.85

Table 5

DIFFERENCES OF SATELLITE FROM TERRESTRIAL ABSOLUTE DATUM POSITIONS

Terrestrial Positions by Kaula (1961)

Meters

Datum	Centroid		Izsak (1965)	Anderle (1965)
NAD	Lat. 30° N	ΔR	-3	+6
	Long. 260° E	$R \cos \varphi \, \Delta\lambda$	+14	-15
		$R \, \Delta \varphi$	+11	-6
ED	Lat. 30° N	ΔR	-41	
	Long. 46° E	$R \cos \varphi \, \Delta\lambda$	-69	
		$R \, \Delta \varphi$	+2	
TD	Lat. 40° N	ΔR	+20	
	Long. 130° E	$R \cos \varphi \, \Delta\lambda$	+34	
		$R \, \Delta \varphi$	-8	

Table 6

NATIONAL GEODETIC SATELLITE PROGRAM ORBITS

Satellite	Launch Date	Inclination	Perigee-Height-Apogee km	
Beacon Explorer B	1964 Oct 10	79.7°	885	1077
Beacon Explorer C	1965 Apr 29	41.2°	939	1318
GEOS-A	1965 3rd Qtr	59°	1100	1500
GEOS-B	1966 2nd-3rd Qtr	80°	1000	1000
PAGEOS	1966 1st-2nd Qtr	90°	3500	4500

COMPARISON OF EVEN ZONAL HARMONICS FROM SATELLITES

	Kozai	King-Hele et al.	Anderle
$\bar{C}_{2,0}$	-484.174	-484.172	-484.194
$\bar{C}_{4,0}$	0.550	0.507	0.507
$\bar{C}_{6,0}$	-0.179	-0.158	-0.219
$\bar{C}_{8,0}$	0.065	-0.107	

Scaling Factor: 10^{-6}

COMPARISON OF SOME TESSERAL HARMONICS FROM SATELLITES

	$\bar{C}_{22}$	$\bar{S}_{22}$	$\bar{C}_{31}$	$\bar{S}_{31}$	$\bar{C}_{33}$	$\bar{S}_{33}$	$\bar{C}_{42}$	$\bar{S}_{42}$	$\bar{C}_{44}$	$\bar{S}_{44}$
Anderle	2.45	-1.52	2.15	0.27	0.58	1.62	0.27	0.67	-0.41	0.34
Guier	2.38	-1.20	1.84	0.21	0.66	0.98	0.42	0.44	-0.21	0.19
Izsak	2.08	-1.25	1.60	-0.04	-0.17	1.40	0.20	0.58	-0.11	0.43

Scaling Factor: 10^{-6}

COMPARISON OF ODD ZONAL HARMONICS FROM SATELLITES

	Kozai	King-Hele et al.	Newton	Anderle
$\bar{C}_{3,0}$	0.963	0.967	1.019	0.984
$\bar{C}_{5,0}$	0.063	0.045	0.002	0.045
$\bar{C}_{7,0}$	0.086	0.114	0.163	0.105
$\bar{C}_{9,0}$	0.012	-0.028	-0.048	

Scaling Factor: 10^{-6}